Rapid catalytic oxidation of arsenite to arsenate in an iron(III)/sulfite system under visible light

Jing Xu [a,b], Wei Ding [a], Feng Wu [a,*], Gilles Mailhot [c], Danna Zhou [d], Khalil Hanna [b,**]

[a] Department of Environmental Science, Hubei Key Lab of Biomass Resource Chemistry and Environmental Biotechnology, School of Resources and Environmental Science, Wuhan University, Wuhan 430079, PR China
[b] Ecole Nationale Supérieure de Chimie de Rennes, CNRS, UMR 6226, 11 Allée de Beaulieu, CS 50837, 35708 Rennes Cedex 7, France
[c] Clermont Université, Université Blaise Pascal-ENSCCF, Institut de Chimie de Clermont-Ferrand (ICCF), BP10448, F-63000 Clermont-Ferrand, France
[d] Faculty of Material Sciences and Chemistry, China University of Geosciences, Wuhan 430074, PR China
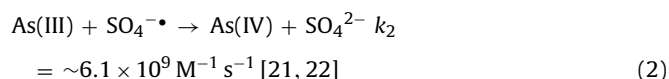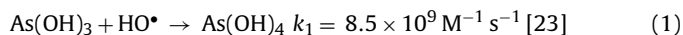
ARTICLE INFO

ABSTRACT

Removal of arsenic in industrial wastewaters proceeds often through oxidation of As(III) to As(V) following by precipitation and/or adsorption. In this work, the catalytic oxidation of As(III) to As(V) in an iron(III)/sulfite system and the removal of As(V) under visible light using sunlight or a light-emitting diode lamp were investigated. Our results show a significant enhancement of efficiency of As(III) oxidation at near-neutral pH, whereas 93% of As(III) was removed from solution by centrifugal treatment after 30 min of irradiation. Mechanism investigations revealed that the pathways of As(III) oxidation at circumneutral pH involved free radicals (mainly HO$^\bullet$, SO$_4^{-\bullet}$ and SO$_5^{-\bullet}$) and ligand-to-metal charge transfer between As(III) and colloidal ferric hydroxide particles. Sequential addition of sulfite could improve the oxidation efficiency for water having high concentrations of As(III) (i.e., 66.7 μM). These results clearly show that the visible light/iron(III)/sulfite system significantly enhances As(III) oxidation. This finding may have promising implications in developing a new cost-effective technology for the treatment of arsenic-containing water using sunlight.

© 2015 Elsevier B.V. All rights reserved.

1. Introduction

Arsenic contamination has drawn much attention worldwide for many years. The distribution of arsenic species determines not only their behavior and toxicity in various environmental media [1,2], but also methods of their removal from contaminated waters and soils [3]. Since the toxicity of inorganic arsenite (As(III)) is higher than that of inorganic arsenate (As(V)), detoxification of arsenic by oxidation of As(III) to As(V) [4–6] is often considered before removing it from industrial wastewater by precipitation, filtration, or adsorption [7,8]. Among the classical oxidants, chlorine, ozone, potassium permanganate (KMnO$_4$), and persulfate (PS) [7–9] have been widely used for As(III) oxidation. Some catalyzed oxidation systems such as Fenton reaction [6,10], metal-activated PS [11], and TiO$_2$ photocatalytic [12,13] systems have been applied to the oxidation of As(III). Moreover, energy (e.g., light

[14,15], ultrasonic waves [16], and electricity [17]) has been utilized to enhance As(III) oxidation. Hydroxyl radical (HO$^\bullet$) [15,18–20], superoxide [13], and sulfate radical (SO$_4^{-\bullet}$) [21,22] are potential species for the oxidation of As(III). In particular, HO$^\bullet$ with As(III) has a very high second-order rate constant (Eq. (1)) at low pH (2–5.6) [23]. Second-order rate constants of the reaction between SO$_4^{-\bullet}$ and As(III) are also very high (Eq. (2)) [21,22]. Therefore, both HO$^\bullet$ and SO$_4^{-\bullet}$ radicals may oxidize As(III).

$$\text{As(OH)}_3 + \text{HO}^\bullet \rightarrow \text{As(OH)}_4 \quad k_1 = 8.5 \times 10^9 \, \text{M}^{-1}\,\text{s}^{-1} \, [23] \tag{1}$$

$$\begin{aligned} \text{As(III)} + \text{SO}_4^{-\bullet} &\rightarrow \text{As(IV)} + \text{SO}_4^{2-} \quad k_2 \\ &= {\sim}6.1 \times 10^9 \, \text{M}^{-1}\,\text{s}^{-1} \, [21, 22] \end{aligned} \tag{2}$$

Although SO$_4^{-\bullet}$-based advanced oxidation processes (S-AOPs) have drawn great attention in recent decades [22,24,25], little is known about the mechanism of As(III) oxidation by S-AOPs and the nature of the reactive oxygen species involved. The system using sulfite (generally expressed as S(IV)) as reactant and iron(II), iron(III), or light as inductor can also produce SO$_4^{-\bullet}$ [26]. Recently, iron(II)/(III)–sulfite systems with or without UV light have been

* Corresponding author. Fax: +86 2768778511.
** Corresponding author. Fax: +33 223238120.
E-mail addresses: fengwu@whu.edu.cn (F. Wu), khalil.hanna@ensc-rennes.fr (K. Hanna).

used to decolorize azo dyes, but dye mineralization in such systems is very poor [27–30]. Although As(III) can be oxidized in such systems with or without UV light [31–33], the possibility of utilizing Fe-sulfite system for rapid As(III) oxidation under visible light (e.g., sunlight) has not been explored. Furthermore, the mechanisms of As(III) oxidation by generated oxysulfur radicals (e.g., $SO_3^{-\bullet}$, $SO_4^{-\bullet}$, and $SO_5^{-\bullet}$) are still unclear. Therefore, the present work aimed to determine the mechanism of As(III) oxidation at circumneutral pH in an iron-catalyzed sulfite system using visible light. In order to determine the role of different oxysulfur radicals in the reaction, radical scavengers, an iron-complexing agent and nitrogen gas were used. Our work may contribute to an understanding of the main mechanisms of As(III) removal using an iron–sulfite system and may aid development of new As(III) decontamination methods driven by visible light.

2. Materials and methods

2.1. Chemicals

Ultrapure water obtained from a water purification system (Liyuan Electric Instrument Co., Beijing, China) was used in the experiments. $NaAsO_2$ (99.5%; Gracia Chemical Technology Co., Ltd., Chengdu, China) was used after 24 h of drying in desiccators. $Na_2HAsO_4 \cdot 7H_2O$ was purchased from Alfa Aesar (Ward Hill, MA). Na_2SO_3 (analytical reagent (AR)) was purchased from Sinopharm Chemical Reagent Co., Ltd. (Shanghai, China) and was used without further purification, the stock solution was freshly prepared before each experiment. *tert*-Butyl alcohol (TBA, AR) was purchased from Shanghai Shiyi Chemicals Reagent Co., Ltd., and ethanol (EtOH, AR) was obtained from Tianjin Kermel Chemical Reagent Co., Ltd. 5,5-Dimethyl-1-pyrroline *N*-oxide (DMPO) was purchased from J&K Scientific Co., Ltd. To prepare 100 mL of Fe(III) stock solution, 0.4g of $Fe_2(SO_4)_3$ (AR; Taishan Chemicals Reagent Co., Ltd.) was weighed into a 100 mL beaker containing 50 mL of ultrapure water and 5 mL of H_2SO_4 solution (98%, Sinopharm Chemical Reagent Co., Ltd). After complete dissolution and cooling, the mixture was diluted to 100 mL with ultrapure water. All the other reagents were analytically pure (except KBH_4 (95%) and formaldehyde (37%)) and were obtained from Sinopharm Chemical Reagent Co., Ltd. All prepared solutions were protected from light and stored at 4 °C.

2.2. Photooxidation reaction system and batch experiments

Batch experiments (except solar irradiation experiments) were conducted in a 500 mL cylindrical, hollow cooling equipment at 25 °C in the dark or under irradiation by four light-emitting diodes (λ = 404 nm; emission spectrum is shown in Fig. S1 in the Supporting information). The irradiation system is described in detail in our previous work [34]. A pH meter (PHS-3C, Aolilong Co., Ltd., Hangzhou, China) and a dissolved oxygen (DO) meter (8403, AZ Instrument Co., Ltd., Taiwan, China) was placed in the beaker to determine the pH and DO values before and during reactions. The solutions were stirred continuously by a magnetic stirrer. Predetermined amounts of As(III) and Fe(III) were diluted in a 500 mL flask and transferred to a beaker after complete mixing. The pH value of the mixture was adjusted to slightly lower than the desired value with diluted NaOH and H_2SO_4 solutions. Fresh Na_2SO_3 solution was added to this reaction solution to reach the desired pH value, and then lamps were switched on. At specified time intervals, a certain amount of the solution sample was collected for analysis. Batch experiments were all conducted under the irradiation of LED lamps unless otherwise stated.

In sunlight-induced oxidation experiments, sunlight was used instead of LED lamps for irradiation, and all other procedures remained the same as in previous batch experiments. Sunlight-induced oxidation experiments were conducted at different times during a day in order to simulate different light intensities as previously reported [35].

In N_2 purging experiments, the top of the cylinder reactor was sealed with a rubber stopper. Purging of solutions with high-purity N_2 (99.99%) was performed for 30 min before reactions and was continued during reactions to ensure that oxygen was excluded.

Iron speciation (i.e., dissolved ion vs. solid form) at various pH values was determined. A 0.1 mM iron(III) solution with initial pH of 2.0 was prepared. The pH was adjusted to desired values, and then 10 mL of the resulting mixture was drawn for centrifugation at 9000 rpm for 15 min. Subsequently, the supernatant was used to determine the concentration of dissolved iron.

In experiments on arsenic removal, samples after reaction were taken and centrifuged for 15 min at 9000 rpm. The supernatant was used to determine the residual concentration of arsenic in solution.

2.3. Analytical methods

Total As(III), As(T) (As(III) + As(V)), and iron species concentrations were determined as explained in our previous works [34,36]. Withdrawn samples were diluted with 1.5% HCl (for As(III) determination) or 5% HCl (for As(T) determination) solution. Sample dilution and pH lowering stopped arsenic oxidation, as proven by experimental results at pH 1 under irradiation; results show negligible oxidation of arsenic under extreme acidic conditions. Moreover, acidic conditions led to the dissolution of iron hydroxide colloids and arsenic species. Arsenic concentration was determined by using hydride generation atomic fluorescence spectrometry (HG-AFS) (Titan Instrument Co., Ltd., Beijing, China). As(III) was determined by using 1.5% HCl−1.5% KBH_4 solution, and As(T) was determined by using 1% thiourea (m V^{-1})−1% ascorbic acid (m V^{-1}) and 5% HCl−2% KBH_4 solutions. Prior to As(T) determination by HG-AFS, thiourea and ascorbic acid were used to reduce As(V) to As(III) [37], then KBH_4 and HCl were used for hydrogenating As(III) to AsH_3 [38]. Fe(II) concentration was determined by spectrophotometry (Shimadzu UV-1601) at 510 nm using 1,10 phenanthroline method [36]. For determination of Fe(III) and then total Fe concentrations, ascorbic acid was used to reduce Fe(III) to Fe(II). The experiment was conducted at least twice, and the error for each sample is shown in figures in the results section.

In sunlight-induced oxidation experiments, a solar power meter (SM206, Shenzhen Sanpometer Ltd., Shenzhen, China) was used to determine the irradiation flux of solar power. To compare the reaction rate constants under different conditions, pseudo-first-order equation was used to fit the kinetic data. The pseudo-first-order equation can be expressed as: $\ln(C/C_0) = -k_{app}t$, where C_0 and C are the concentrations at initial time and any reaction time t, respectively. k_{app} (min^{-1}) was calculated from the slope of the plots of $\ln(C/C_0)$ vs. t. Due to the complexity of oxidation mechanisms and fast consumption of sulfite in the iron(III)/sulfite–visible light system, the equation applied only to the data obtained in the first 5 min.

3. Results and discussion

3.1. Effect of visible irradiation

As shown in Fig. 1, As(III) was oxidized slowly in the iron(III)/sulfite system at circumneutral pH in the dark. The oxidation efficiency was significantly improved under LED lamps irradiation: ∼74% of As(III) was oxidized within 10 min. Blank experiments (Fig. 1) showed no As(III) oxidation in the absence of Fe(III), indicating that sulfite did not generate oxysulfur radicals
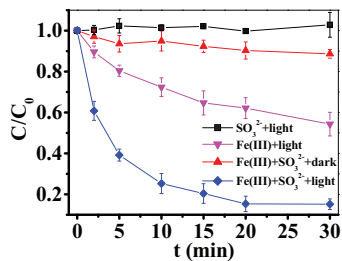
Fig. 1. Changes in As(III) concentration over time in different systems. Initial conditions: pH 6, [As(III)] = 6.67 μM, [Fe(III)] = 0.1 mM, [Na$_2$SO$_3$] = 0.1 mM.

Fig. 2. Changes in As(III) concentration over time under solar power. Solid lines are fitted to a pseudo-first-order curve for the first 5 min. Initial conditions: pH 6, [As(III)] = 6.67 μM, [Fe(III)] = 0.1 mM, [Na$_2$SO$_3$] = 0.1 mM.

Fig. 3. Effect of sulfite dosage on the initial apparent rate constant of As(III) oxidation (k_{app}). The curve is only a visual guide. Initial conditions: pH 6, [As(III)] = 6.67 μM, [Fe(III)] = 0.1 mM.

via direct photolysis. However, ∼45% of As(III) was oxidized in the presence of Fe(III) in the absence of sulfite within 30 min. Colloidal ferric hydroxides (CFH) can form at near-neutral pH conditions (See Table S1) and thus sorb As(III) through surface complexation [39,40]. As(III) can then be oxidized by electron transfer from As(III) to Fe(III) induced by radiation absorption via ligand-to-metal charge transfer (LMCT), as previously reported [34]. Consequently, the decrease in total As(III) concentration determined after sample acidification (Fig. 1) may be due to radical oxidation pathway of As(III) and also adsorption on CFH followed by oxidation. The difference between the total As concentration and total As(III) concentration corresponds to the oxidation of As(III) to As(V) (Fig. S2).

Because the treatment of arsenic containing wastewater must include not only the oxidation of As(III) to As(V) but also the removal of final product (i.e., As(V)), centrifugation at 9000 rpm for 15 min was conducted to assess the removal of arsenic from aqueous phase. After photo-iron(III)/sulfite treatment, the most of As(III) was oxidized to the less soluble form As(V), that was then removed by precipitation/adsorption to CFH. It should be noted that both As(V) and As(III) were removed by combining oxidation and centrifugation process. Approximately 93% of total arsenic were removed from solution (Table S2), which is close to the amount of Fe(III) (∼ 96% of 0.1 mM) precipitated at pH 6 (Table S1).

In the iron(II)/sulfite system, DO takes part in the oxidation of Fe(II) and sulfite via Eqs. (4) and (7) [41,42]. Here, iron recycling and generation of oxysulfur radicals rely on the presence of oxygen (Eqs. (5)–(8)) [43]. The variation of DO content in the iron(III)/sulfite system at initial pH of 6 between dark and light conditions was compared (Fig. S3a). In the dark condition, the DO content slightly increased because of reoxygenation. Under irradiation, the DO content sharply declined, suggesting formation of free radicals (Eqs. (7)–(10)) and oxidation of reduced Fe(II) (Eq. (4)), which would increase the efficiency of oxidation. In the latter stage of the reaction, sulfite consumption (Fig. S3b) and reoxygenation may explain the small increase in DO content.
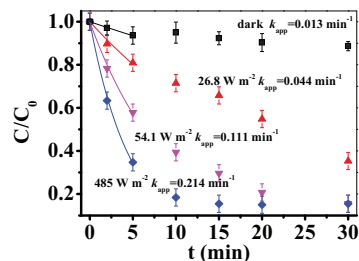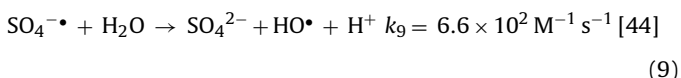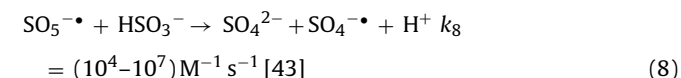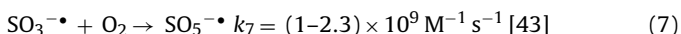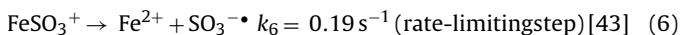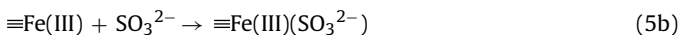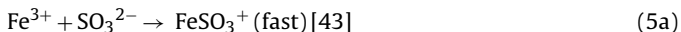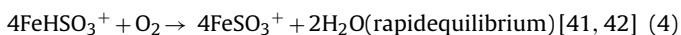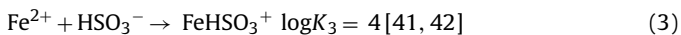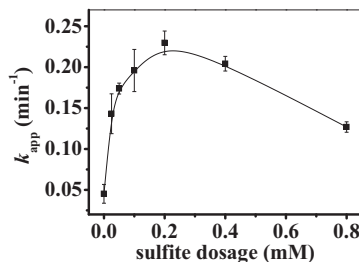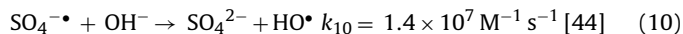
$$Fe^{2+} + HSO_3^- \rightarrow FeHSO_3^+ \quad \log K_3 = 4 \, [41, 42] \tag{3}$$

$$4FeHSO_3^+ + O_2 \rightarrow 4FeSO_3^+ + 2H_2O \, (rapid\,equilibrium) \, [41, 42] \tag{4}$$

$$Fe^{3+} + SO_3^{2-} \rightarrow FeSO_3^+ \, (fast) \, [43] \tag{5a}$$

$$\equiv Fe(III) + SO_3^{2-} \rightarrow \equiv Fe(III)(SO_3^{2-}) \tag{5b}$$

$$FeSO_3^+ \rightarrow Fe^{2+} + SO_3^{-\bullet} \quad k_6 = 0.19 \, s^{-1} \, (rate\text{-}limiting\,step) \, [43] \tag{6}$$

$$SO_3^{-\bullet} + O_2 \rightarrow SO_5^{-\bullet} \quad k_7 = (1\text{--}2.3) \times 10^9 \, M^{-1} \, s^{-1} \, [43] \tag{7}$$

$$SO_5^{-\bullet} + HSO_3^- \rightarrow SO_4^{2-} + SO_4^{-\bullet} + H^+ \quad k_8$$
$$= (10^4\text{--}10^7) \, M^{-1} \, s^{-1} \, [43] \tag{8}$$

$$SO_4^{-\bullet} + H_2O \rightarrow SO_4^{2-} + HO^\bullet + H^+ \quad k_9 = 6.6 \times 10^2 \, M^{-1} \, s^{-1} \, [44] \tag{9}$$

$$SO_4^{-\bullet} + OH^- \rightarrow SO_4^{2-} + HO^\bullet \quad k_{10} = 1.4 \times 10^7 \, M^{-1} \, s^{-1} \, [44] \tag{10}$$
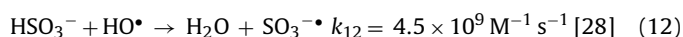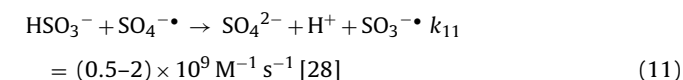
The pH variation relative to the DO content in the dark differed from that under light conditions (Fig. S3c). The pH significantly changed only under irradiation, decreasing sharply in the first 10 min and then very slowly at a later stage because of sulfite consumption (Fig. S3b). The decrease in pH may be explained by Eq. (8), thereby corroborating the formation of oxidizing radical species.

To verify whether the solar power can also promote As(III) oxidation in the iron(III)/sulfite system, experiments were performed under three different intensities of sunlight. The initial pseudo-first-order apparent rate constants k_{app} (min^{-1}) show that As(III) can undergo oxidation in the iron(III)/sulfite system under solar irradiation (Fig. 2). Under an average solar power of 26.8 W m^{-2}, approximately 64% of As(III) was oxidized in 30 min, whereas the efficiency of As(III) photooxidation was enhanced to ∼81% within 10 min under an average solar power of 485 W m^{-2}.

3.2. Effect of sulfite dosage on As(III) oxidation

Different amounts of sulfite were used to investigate the effect of sulfite dosage on As(III) oxidation at pH 6. k_{app} values, determined as previously mentioned, were plotted against sulfite dosage in Fig. 3. k_{app} values increased initially with the increase in sulfite dosage, reached a maximum value at 0.2 mM, and then decreased. According to Eqs. (5)–(10), sulfite–iron(III) complexes can undergo chain reactions that generate oxysulfur radicals and HO$^\bullet$, and increasing the sulfite concentration can improve the initial rate of oxidation. According to Eqs. (11) and (12), however, the generated radicals SO$_4^{-\bullet}$ and HO$^\bullet$ can be scavenged by sulfite when it is used at much higher concentrations.

$$HSO_3^- + SO_4^{-\bullet} \rightarrow SO_4^{2-} + H^+ + SO_3^{-\bullet} \quad k_{11}$$
$$= (0.5\text{--}2) \times 10^9 \, M^{-1} \, s^{-1} \, [28] \tag{11}$$

$$HSO_3^- + HO^\bullet \rightarrow H_2O + SO_3^{-\bullet} \quad k_{12} = 4.5 \times 10^9 \, M^{-1} \, s^{-1} \, [28] \tag{12}$$
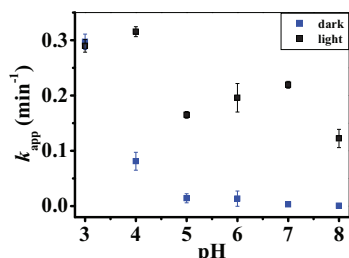
Fig. 4. Effect of initial pH value on the initial apparent rate constant of As(III) oxidation (k_{app}) under dark and light conditions. Initial conditions: [As(III)] = 6.67 μM, [Fe(III)] = 0.1 mM, [Na$_2$SO$_3$] = 0.1 mM.
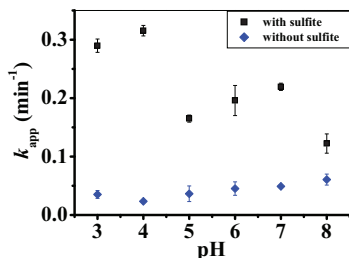

Fig. 5. Effect of the presence of sulfite on the initial apparent rate constant of As(III) oxidation (k_{app}) at various initial pH values. Initial conditions: [As(III)] = 6.67 μM, [Fe(III)] = 0.1 mM, [Na$_2$SO$_3$] = 0.1 mM.

Variations of DO content and pH with the sulfite dosage were also determined (Fig. S4a and b). The rate of DO depletion increased with the increase in sulfite dosage. When [SO$_3^{2-}$] = 0.8 mM, the DO content decreased rapidly from 6.68 to 0 mg L^{-1} within 10 min. According to Eqs. (4) and (7), the depletion of DO observed at high dosage of sulfite could affect the generation of radicals and thus the rate of oxidation. Similarly, the pH decreased with increasing sulfite concentration, probably because of the generation of protons through Eqs. (8) and (11).

3.3. Effect of pH value on As(III) oxidation

The effect of pH on As(III) oxidation kinetics with or without light was investigated over a wide pH range (3–8). Without irradiation, As(III) oxidation was significant at pH 3, and then k_{app} decreased with increase of pH (results of k_{app} are shown in Fig. 4). Irradiation did not affect k_{app} significantly at pH 3, however, in the pH range of 4–8, k_{app} was significantly enhanced by irradiation. The effect of the presence of sulfite is also different at various pH values (Fig. 5). In the absence of sulfite, k_{app} increased slightly with increasing pH. In the presence of sulfite, k_{app} is significantly higher than that in the absence of sulfite over the whole pH range investigated. To explain this pH-dependence, the mechanisms of As(III) oxidation under light conditions at 3 different pH values (i.e., pH 3, 6 and 8) were investigated and presented in the following paragraph.

3.4. Oxidation mechanisms under light conditions

Electron spin resonance (ESR) spectroscopy, radical scavenging and nitrogen purging experiments were conducted to determine the nature of radicals involved at each pH value. In the presence of DMPO compound used in ESR experiments, SO$_3^{•-}$ seems to be the predominant radical in the first stage of radical chain reactions (see Fig. S5). However, in the absence of DMPO (as in our reaction medium) and in the presence of oxygen, SO$_3^{•-}$ can be easily oxidized to SO$_5^{•-}$ (Eq. (7)), thereby considerably mitigating the contribution of SO$_3^{•-}$ in our system.
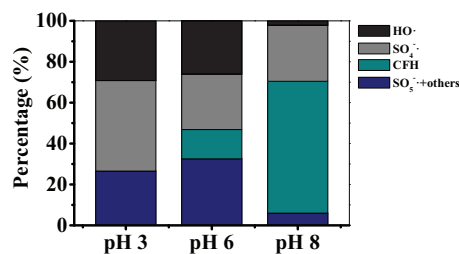

Fig. 6. Contribution of different pathways to As(III) oxidation at various initial pH values.

In the scavenging experiments TBA was used to capture HO$^{•}$ ($k_{TBA,HO^{•}}$ = (3.8–7.6) × 10^8 M^{-1} s^{-1} [45]), whereas EtOH was used to capture HO$^{•}$ and SO$_4^{-•}$ ($k_{EtOH,HO^{•}}$ = (1.8–2.8) × 10^9 M^{-1} s^{-1} [46], $k_{EtOH,SO4}^{-•}$ = (1.6–6.2) × 10^7 M^{-1} s^{-1} [47,48]). N$_2$ was used to eliminate the effect of oxygen. Supposing that radicals (HO$^{•}$ or SO$_4^{•-}$) and LMCT process are mainly involved in As oxidation, their contributions were calculated by using k_{app} value estimated for each condition (see Table S3). Indeed, the contribution of HO$^{•}$ was obtained from the difference in k_{app} with and without addition of TBA, and that of SO$_4^{•-}$ was obtained from the difference in k_{app} with EtOH and with TBA. Generally, nitrogen gas purging system can eliminate the effect of oxygen and thus reduce the formation of radicals, and therefore the contribution of LMCT oxidation was obtained from the k_{app} estimated under N$_2$ purging (Fig. 6). As k_{app} in the presence of EtOH was higher than that under N$_2$ purging, we may expect the generation of various radicals species such as SO$_5^{•-}$. The likelihood of SO$_5^{•-}$ participation in As(III) oxidation is also supported by the fact that EtOH cannot effectively scavenge SO$_5^{•-}$ (rate constant < 1 × 10^3 M^{-1} s^{-1} [49]).

The contributions of HO$^{•}$ and SO$_4^{-•}$ decreased with pH increasing. For SO$_4^{-•}$, this observation is consistent with the classical Fenton system, in which the performance of radical-involved oxidation process decays with pH increasing due to the precipitation of ferrous or ferric ions [50,51]. Indeed, the aqueous concentrations of Fe(II) decreased with pH increasing (Fig. S6), consistently with the distribution diagram of Fe(II) species vs. pH [52]. For HO$^{•}$, part of dissolved Fe(III) can be complexed with OH$^-$, forming Fe(III)-OH complex under acidic conditions and then generating HO$^{•}$ according to Eq. (13). When pH increases, dissolved Fe precipitated causing a decrease of HO$^{•}$ generation.

$$FeOH^{2+} + hv \rightarrow Fe^{2+} + HO^{•} \text{ [53]} \tag{13}$$

On the other hand, generation of HO$^{•}$ through SO$_4^{-•}$ under acidic conditions is supposed to be lower than under basic conditions according to Eqs. (9) and (10). However, the latter did not affect significantly the overall generation rate.

Under N$_2$ purging, As(III) oxidation was observed at all tested pH values. At near-neutral conditions, Fe(III) mainly occurred as CFH and As(III)-sorbed species may undergo oxidation through LMCT. As CFH formed more easily with the increase in pH, more As(III) underwent oxidation at pH 8 than at pH 6. It is noteworthy that at pH 3 (dark) under nitrogen purging, As(III) oxidation was not completely inhibited (Fig. S7). This was not caused by LMCT because of the absence of visible light. According to Eq. (6), SO$_3^{•-}$ generation is not dependent on the presence of oxygen, whereas the occurrence of SO$_3^{•-}$ can generate dithionate (S$_2$O$_6^{2-}$) (Eq. (14)) [54] and then oxidize As(III). To confirm this hypothesis, Na$_2$S$_2$O$_5$ was used as the source of S$_2$O$_6^{2-}$. In the presence of oxygen, Na$_2$S$_2$O$_5$ is easily oxidized to Na$_2$S$_2$O$_6$. In order to exclude other factors, Fe(III) and irradiation were removed in this experiment. As shown in Fig. S8, a small fraction of As(III) was oxidized, suggesting that As(III) oxidation was partly caused by S$_2$O$_6^{2-}$. Additional experiments conducted at pH 6 and 8 under dark anoxic conditions (Fig. S7)
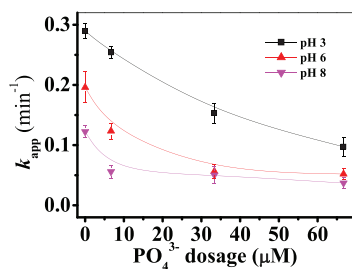
Fig. 7. Inhibitory effect of phosphate at different concentrations on the initial apparent rate constant of As(III) oxidation (k_{app}) at various pH values. The curves are only a visual guide. Initial conditions: [As(III)] = 6.67 μM, [Fe(III)] = 0.1 mM, [Na$_2$SO$_3$] = 0.1 mM.

showed a small fraction oxidized at pH 6 and negligible oxidation at pH 8, confirming the role of $S_2O_6^{2-}$ in As(III) oxidation at pH 6. Under acidic conditions, the presence of oxygen had no obvious influence on $S_2O_6^{2-}$ generation [55], suggesting that $S_2O_6^{2-}$ contributes to As(III) oxidation even under acid oxic conditions. However, $SO_3^{\bullet-}$ tends to react with DO under near-neutral and basic conditions (Eq. (7)), preventing the generation of $S_2O_6^{2-}$.

$$SO_3^{-\bullet} + SO_3^{-\bullet} \rightarrow S_2O_6^{2-} \quad k_{14} = 1.8 \times 10^8 \, M^{-1} \, s^{-1} \, [54] \quad (14)$$
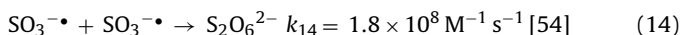
Because the contributions of $S_2O_6^{2-}$ (<6% at pH 3) and of LMCT (due to the low amount of CFH at low pH) are supposed to be low, these two pathways were ignored in our calculations at pH 3 (Fig. 6). In addition, the contribution of CFH must be considered as roughly estimated under acid or neutral conditions (Fig. 6), because the role of $S_2O_6^{2-}$ (even minor) has not been taken into account.

To obtain further insights into the oxidation mechanism in the iron(III)/sulfite system, we investigated effect of phosphate at different pH. Estimated k_{app} values for each condition are plotted against phosphate concentration in Fig. 7. The presence of phosphate led to a decrease in k_{app} regardless of the pH tested. As PO_4^{3-} has an atomic structure similar to that of arsenic, it can compete with As(III) for adsorption onto CFH formed at near-neutral pH and can completely inhibit As(III) oxidation [34]. However in iron(III)/sulfite system, phosphate could not completely inhibit oxidation at pH 6 and 8, suggesting that other oxidation processes may occur under near-neutral conditions. Moreover, the decrease in k_{app} at pH 3 implies that phosphate may also compete with sulfite in complexing with dissolved iron. Inspection of Table S3 and Fig. 7 reveals that the contribution of LMCT at pH 6 is smaller than the inhibition extent of As oxidation in the presence of phosphate. This observation suggests that phosphate may inhibit As(III) oxidation by affecting both LMCT process and chain reactions of dissolved Fe. At pH 8, no significant difference was observed probably because of the low percentage of dissolved Fe at this pH value.

3.5. Sequential experiments for higher-scale applications

Sequential experiments were performed with multiple additions of As(III) and sulfite to evaluate the catalytic capacity of iron(III)/sulfite system in arsenic removal. An experiment using multiple additions of sulfite was also conducted on water contaminated with a high concentration of arsenic.

3.5.1. Sequential addition of As(III) and arsenic(III)/sulfite

A As(III) solution or As(III)–sulfite mixture was sequentially added to reaction solution every 20 min (Fig. 8). Generally, the extent of oxidation decreased in both cases, but runs with additional sulfite showed higher efficiency in arsenic oxidation. In contrast to Fe, which is recycled under irradiation (i.e., reduction to Fe(II) and then oxidation to Fe(III)), sulfite is not recyclable as it irreversibly transforms into sulfate. Therefore, additional sulfite
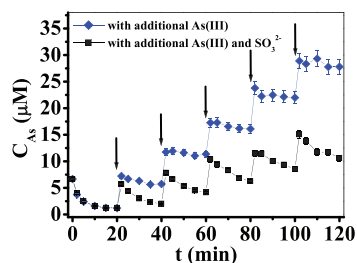

Fig. 8. Changes in As(III) concentration over time in sequential experiments. Initial conditions: pH 6, [As(III)] = 6.67 μM, [Fe(III)] = 0.1 mM, [Na$_2$SO$_3$] = 0.1 mM, multiple additions of 2.5 mL 1.34 mM As(III) and 2.5 mL 20 mM SO$_3^{2-}$ solutions every 20 minutes.
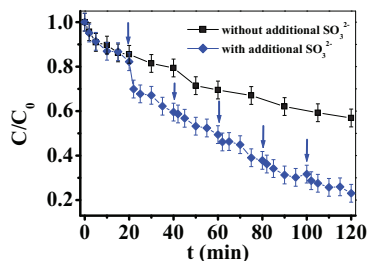

Fig. 9. Changes in As(III) concentration over time at high arsenic levels. Initial conditions: pH 6, [As(III)] = 66.7 μM, [Fe(III)] = 0.1 mM, [Na$_2$SO$_3$] = 0.1 mM, multiple additions of 2.5 mL 20 mM SO$_3^{2-}$ solution. Arrows indicate the time of sulfite addition.

is necessary to promote sequential treatment. In the experiment without sequential addition of sulfite, the oxidation of additional As(III) might be caused by LMCT process. In both cases, the generated As(V) can sorb onto CFH and then saturate the reactive surface sites, thus decreasing the overall oxidation efficiency.

3.5.2. High initial concentration of As(III)

In some regions, the maximum level of As contamination reach some mg L^{-1} concentrations [56]. Therefore, the removal of high concentrations of arsenic merits investigation from an environmental point of view. Reactions with high As(III) concentration (66.7 μM = 5 mg L^{-1}) were conducted (results are shown in Fig. 9). Without additional sulfite, approximately 43% of As(III) was oxidized after 120 min reaction, while up to 77% was oxidized when 2.5 mL of 20 mM sulfite solution was added to reaction solution every 20 min. As mentioned above, the consumption of sulfite lowered the efficiency of As(III) oxidation; thus, additional sulfite was needed to enable removal of higher amounts of arsenic. Furthermore, the first addition of sulfite significantly improved As removal, but this effect became less important with further additions probably because of precipitation of iron and adsorption of generated As(V) on CFH.

4. Conclusions

Our results showed the high efficiency of the iron(III)/sulfite system in As(III) removal under visible light and sunlight. Our findings suggested multiple pathways to explain the oxidation of As(III) into As(V) in iron(III)/sulfite system. We have notably demonstrated that the mechanism of As(III) oxidation involved hydroxyl and oxysulfur radicals. CFH formed at near-neutral pH can sorb and then oxidize As(III) by electron transfer from As(III) to Fe(III) induced by absorption of radiation during LMCT process. Under acidic and anoxic conditions, $S_2O_6^{2-}$ can also be formed and thus contribute to As(III) oxidation.

A high dosage of sulfite can inhibit As(III) oxidation, but a deficiency in sulfite may decrease the oxidation rate. Experiments using multiple additions of As(III) or arsenic(III)–sulfite mixtures showed the importance of sulfite addition in increasing the efficiency of As(III) removal. The visible light/iron(III)/sulfite system and centrifugal treatment could effectively remove arsenic under near-neutral conditions. All these results imply that the sunlight/iron(III)/sulfite system is a cost-effective process for arsenic removal in contaminated waters.

Acknowledgements

Appendix A. Supplementary data

Supplementary data associated with this article can be found, in the online version, at http://dx.doi.org/10.1016/j.apcatb.2015.12.033.

References

[1] J.H. Huang, E. Matzner, Sci. Total Environ. 377 (2) (2007) 308–318.
[2] C.K. Jain, I. Ali, Water Res. 34 (17) (2000) 4304–4312.
[3] M. Sadiq, Water Air Soil Pollut. 93 (1–4) (1997) 117–136.
[4] Z. Wang, R.T. Bush, L.A. Sullivan, C. Chen, J. Liu, Environ. Sci. Technol. 48 (7) (2014) 3978–3985.
[5] Z. Wang, R.T. Bush, L.A. Sullivan, J. Liu, Environ. Sci. Technol. 47 (12) (2013) 6486–6492.
[6] S.J. Hug, O. Leupin, Environ. Sci. Technol. 37 (12) (2003) 2734–2742.
[7] M. Bissen, F.H. Frimmel, Acta Hydrochimica et Hydrobiol. 31 (2) (2003) 97–107.
[8] T.S. Choong, T.G. Chuah, Y. Robiah, F.G. Koay, I. Azni, Desalination 217 (1) (2007) 139–166.
[9] S. Nishida, M. Kimura, J. Chem. Soc. Dalton Trans. 2 (1989) 357–360.
[10] Z. Wang, R.T. Bush, J. Liu, Chemosphere 93 (9) (2013) 1936–1941.
[11] L. Zhou, W. Zheng, Y. Ji, J. Zhang, C. Zeng, Y. Zhang, Q. Wang, X. Yang, J. Hazard. Mater. 263 (2013) 422–430.
[12] S. Yoon, J.H. Lee, Environ. Sci. Technol. 39 (24) (2005) 9695–9701.
[13] J. Ryu, W. Choi, Environ. Sci. Technol. 40 (22) (2006) 7034–7039.
[14] M.T. Emett, G.H. Khoe, Water Res. 35 (3) (2001) 649–656.
[15] S.J. Hug, L. Canonica, M. Wegelin, D. Gechter, U. von Gunten, Environ. Sci. Technol. 35 (10) (2001) 2114–2121.
[16] B. Neppolian, A. Doronila, M. Ashokkumar, Water Res. 44 (12) (2010) 3687–3695.
[17] J. Sánchez, B. Butter, B.L. Rivas, L. Basáez, P. Santander, J. Appl. Electrochem. 45 (2) (2015) 151–159.
[18] B.D. Kocar, W.P. Inskeep, Environ. Sci. Technol. 37 (8) (2003) 1581–1588.
[19] S.H. Yoon, J.H. Lee, J. Ind. Eng. Chem. 13 (1) (2007) 97–104.
[20] P.K. Dutta, S.O. Pehkonen, V.K. Sharma, A.K. Ray, Environ. Sci. Technol. 39 (6) (2005) 1827–1834.
[21] R. Woods, I.M. Cutoff, E.J. Meehan, J. Am. Chem. Soc. 85 (16) (1963) 2385–2390.
[22] R. Woods, I.M. Kolthoff, E.J. Meehan, J. Am. Chem. Soc. 85 (21) (1963) 3334–3337.
[23] U.K. Klaning, B.H.J. Bielski, K. Sehested, Inorg. Chem. 28 (14) (1989) 2717–2724.
[24] S.Y. Nishida, M. Kimura, Inorg. Chim. Acta 174 (1990) 231–235.
[25] B. Neppolian, E. Celik, H. Choi, Environ. Sci. Technol. 42 (16) (2008) 6179–6184.
[26] Y. Guo, X. Lou, C. Fang, D. Xiao, Z. Wang, J. Liu, Environ. Sci. Technol. 47 (19) (2013) 11174–11181.
[27] L. Chen, X. Peng, J. Liu, J. Li, F. Wu, Ind. Eng. Chem. Res. 51 (42) (2012) 13632–13638.
[28] L. Zhang, L. Chen, M. Xiao, L. Zhang, F. Wu, L. Ge, Ind. Eng. Chem. Res. 52 (30) (2013) 10089–10094.
[29] D. Zhou, L. Chen, C. Zhang, Y. Yu, L. Zhang, F. Wu, Water Res. 57 (2014) 87–95.
[30] D. Zhou, H. Zhang, L. Chen, J. Chem. Technol. Biotechnol. 90 (5) (2014) 775–779.
[31] T. Nishimura, Q. Wang, Y. Umetsu, in: J.E. Dutrizac, G.B. Harris (Eds.), Iron Control and Disposal, CIM, Ottawa, Montreal, Canada, 1996, pp. 535–548.
[32] G.H. Khoe, M. Zaw, U.S. Patent No. 6,558,556. Washington, DC: U.S. Patent and Trademark Office (2003).
[33] W. Zhang, P. Singh, D.M. Muir, Proc. Minor Elem. (2000) 333–343.
[34] J. Xu, J. Li, F. Wu, Y. Zhang, Environ. Sci. Technol. 48 (1) (2013) 272–278.
[35] S. Sakthivel, B. Neppolian, M.V. Shankar, B. Arabindoo, M. Palanichamy, V. Murugesan, Sol. Energ. Mater. Sol. Cells 77 (1) (2003) 65–82.
[36] Y. Wang, J. Xu, J. Li, F. Wu, J. Hazard. Mater. 260 (2013) 255–262.
[37] C. Ren, H. Peng, W. Huang, Y. Wang, F. Wu, Fresen. Environ. Bull. 20 (4) (2011) 1069–1074.
[38] C.G. Yuan, K. Zhang, Z. Wang, G. Jiang, J. Anal. Atom. Spectrom. 25 (10) (2010) 1605–1611.
[39] L.C. Roberts, S.J. Hug, T. Ruettimann, M.M. Billah, A.W. Khan, M.T. Rahman, Environ. Sci. Technol. 38 (1) (2004) 307–315.
[40] B.A. Manning, S.E. Fendorf, S. Goldberg, Environ. Sci. Technol. 32 (16) (1998) 2383–2388.
[41] Y. Zhang, J. Zhou, C. Li, S. Guo, G. Wang, Ind. Eng. Chem. Res. 51 (3) (2012) 1158–1165.
[42] I. Grgićc, P. Marjeta, B. Mirko, J. Atmos. Chem. 33 (1) (1999) 89–102.
[43] D.T.F. Kuo, D.W. Kirk, C.Q. Jia, J. Sulfur Chem. 27 (5) (2006) 461–530.
[44] P.H. Wine, Y. Tang, R.P. Thorn, J.R. Wells, D.D.J. Davis, Geophys. Res.-Atmos. 94 (D1) (1989) 1085–1094.
[45] G.P. Anipsitakis, D.D. Dionysiou, Environ. Sci. Technol. 38 (13) (2004) 3705–3712.
[46] G.E. Adams, J.W. Boag, B.D. Michael, Trans. Faraday Soc. 61 (1965) 1417–1424.
[47] H. Eibenberger, S. Steenken, P. O'Neill, D. Schulte-Frohlinde, J. Phys. Chem. 82 (6) (1978) 749–750.
[48] L. Dogliotti, E. Hayon, J. Phys. Chem. 71 (8) (1967) 2511–2516.
[49] E. Hayon, A. Treinin, J. Wilf, J. Am. Chem. Soc. 94 (1) (1972) 47–57.
[50] X. Xue, K. Hanna, M. Abdelmoula, N. Deng, Appl. Catal. B-Environ. 89 (3) (2009) 432–440.
[51] X. Xue, K. Hanna, N. Deng, J. Hazard. Mater. 166 (1) (2009) 407–414.
[52] D.W. King, Environ. Sci. Technol. 32 (19) (1998) 2997–3003.
[53] F. Wu, N.S. Deng, Chemosphere 41 (8) (2000) 1137–1147.
[54] W. JohnáMcElroy, J. Chem. Soc. Faraday Trans. 88 (11) (1992) 1525–1530.
[55] C. Brandt, R. Van Eldik, Atmos. Environ. 31 (24) (1997) 4247–4249.
[56] S.R. Panthi, S. Sharma, A.K. Mishra, J. Sci. Eng. Technol. 2 (1) (2006) 1–11.